Available online at www.sciencedirect.com
ScienceDirect
Journal of Solid State Chemistry 180 (2007) 583–588
JOURNAL OF SOLID STATE CHEMISTRY
www.elsevier.com/locate/jssc

Construction of a double-layered tetrahedral network within a perovskite host: Two-step route to the alkali-metal-halide layered perovskite, $(Li_xCl)LaNb_2O_7$

Liliana Viciu, Thomas A. Kodenkandath, John B. Wiley*

Department of Chemistry and the Advanced Materials Research Institute, University of New Orleans, LA 70148-2820, USA

Received 21 June 2006; received in revised form 1 November 2006; accepted 6 November 2006
Available online 17 November 2006

Abstract

A two-step topotactic route is used to construct lithium halide layers within a perovskite host. Initially $RbLaNb_2O_7$ is converted to $(CuCl)LaNb_2O_7$ by ion exchange and then reductive intercalation with *n*-butyllithium is used to form $(Li_xCl)LaNb_2O_7$. The copper metal byproduct from the reduction step is removed by treatment with iodine. Rietveld refinement of neutron powder diffraction data revealed that an alkali-halide double layer with LiO_2Cl_2 tetrahedra forms between the perovskite slabs. Compositional studies indicate that the range for x in $(Li_xCl)LaNb_2O_7$ is $2 \leqslant x < 4$, which appears consistent with the neutron data where only one lithium site was found in the structure.

Keywords: Layered compounds; Perovskite; Topochemical

1. Introduction

Strategies based on topochemical reaction schemes offer the potential for the rational design of new materials. Both ion exchange and intercalation methods are valuable tools in the topochemical manipulation of compounds. Simple ion exchange methods allow for the replacement of select cations (or anions) within a compound and intercalation methods, either oxidative or reductive, allow for the insertion of various ions as the valence of the host compound is varied. The potential of combining such reactions for deliberate formation of specific structures is especially exciting. Recent work in this area involving multistep reaction strategies has resulted in a series of interesting compounds [1]. These efforts have produced a variety of oxides including those that are mixed valent [2], cation deficient [3], or contain intergrowths of metal-halide/metal-oxide layers [4]. Building on methods for the formation of transition-metal-halide arrays within perovskite hosts (intergrowths) [5], we developed a multistep approach for preparing alkali-metal-halide perovskites of the form $(A_xCl)LaNb_2O_7$ (A = Li, Na). Our preliminary results for these systems were reported previously [6]. Herein we present a detailed study on the synthesis and purification of $(Li_xCl)LaNb_2O_7$ along with structural characterization. This compound serves to illustrate the utility of multistep reaction strategies in the rational approach to new materials.

2. Experimental section

2.1. $RbLaNb_2O_7$ and $(CuCl)LaNb_2O_7$

$RbLaNb_2O_7$ was prepared by mixing together stoichiometric quantities of preheated (1050 °C/12 h) La_2O_3 (Alfa, 99.99%) and Nb_2O_5 (Alfa, 99.9985%) and a 25% molar excess Rb_2CO_3 (Alfa, 99%). The excess of Rb_2CO_3 was added to balance that which was lost as the oxide due to volatilization. The mixture was annealed for 12 h at 850 °C followed by an additional thermal treatment at 1050 °C for 24 h [7]. The product was washed with distilled water and dried at 150 °C overnight. $(CuCl)LaNb_2O_7$ was prepared by a single-step ion-exchange reaction between anhydrous

*Corresponding author. Fax: +1 504 280 6860.
E-mail address: jwiley@uno.edu (J.B. Wiley).

0022-4596/$ - see front matter © 2006 Elsevier Inc. All rights reserved.
doi:10.1016/j.jssc.2006.11.014

$CuCl_2$ (Alfa, 99%) and $RbLaNb_2O_7$ in a 2:1 molar ratio [5]. The reaction was carried out in a sealed, evacuated ($<10^{-3}$ Torr) Pyrex tube at 325 °C. After 7 days, the dark green product was washed with water to eliminate the excess of copper chloride and the rubidium byproduct and then dried at 150 °C for 2 h.

2.2. Lithium intercalation to produce $(Li_xCl)LaNb_2O_7$

n-BuLi was used to intercalate lithium into (CuCl)LaNb_2O_7. The copper oxyhalide (0.3–0.6 g) was loaded into a screw-cap scintillation vial fitted with TFE/silicone septa and sealed under argon. A large excess *n*-BuLi (ACROS, 1.6 M solution in hexane), corresponding to a molar ratio of 12:1 for *n*-BuLi:$(CuCl)LaNb_2O_7$, was then added via a syringe. The powder immediately turned black on addition of the lithium reagent. After 24 h of stirring at room temperature, the solid was collected using a Schlenk funnel, washed with copious amounts of anhydrous hexanes (water <0.002, Aldrich), and dried under vacuum. The product is air sensitive and was therefore routinely handled and stored in an argon-filled dry box.

The above preparation produces $(Li_xCl)LaNb_2O_7$ combined with an amorphous copper metal impurity. Methods were developed to remove the copper. The procedure initially involves the oxidation of copper metal with iodine (EM Science, 99.8%). The black $(Li_xCl)LaNb_2O_7$/Cu mixture (0.5–0.8 g) was combined with I_2 (2–3 g) in a sealed evacuated Pyrex tube (ca. 15 ml volume) and heated at 150 °C for 24 h. X-ray analysis of the resulting white powder showed the presence of CuI. No evidence for LiI was seen, though this compound presumably formed on the oxidation of $(Li_xCl)LaNb_2O_7$. The CuI, along with any LiI, was then removed with acetonitrile that had been dried over P_2O_5. Sometimes several oxidation cycles with iodine were needed to remove all the copper from a sample. The wash step was carried out in a Schlenk funnel before the sample was dried under vacuum. The color of the final product is very light gray. Energy dispersive spectroscopy (EDS) analysis determined that all of the copper was removed from the sample and that the Cl, La, and Nb content was maintained. ICP analysis on lithium showed the final composition to be $(Li_{2.01(1)}Cl)LaNb_2O_7$.

The copper-free $(Li_{2.01(1)}Cl)LaNb_2O_7$ product was used for further lithium intercalation. $(Li_2Cl)LaNb_2O_7$ and *n*-BuLi were combined as described above in molar ratios 1:1, 1:2, 1:3, 1:12 and stirred for 24 h at room temperature. A significant color change to metallic blue (blue bronze) was observed after the addition of the reducing agent. The products were collected on a filtration frit under an argon atmosphere, washed with anhydrous hexanes (water <0.002% Aldrich), and dried under vacuum. ICP analysis revealed the lithium composition of 2.48, 3.28, 3.32, and 3.55 corresponding for 1:1, 1:2, 1:3, and 1:12 molar ratios, respectively. The maximum amount of lithium found after a second intercalation was also 3.55 (molar ratio of 1:12). Note that special handling is needed for all these materials; the intercalated lithium samples are extremely air/moisture sensitive and an almost instantaneous color change occurs when exposed to air.

Large samples, typically 3–4 g, were needed for neutron diffraction studies. Samples were prepared in small quantities (<0.5 g) and combined to make the larger samples. Because of the high air sensitivity of these materials and the potential loss of samples, the number of processing steps was kept to a minimum. In spite of this, samples treated four times with iodine still contained some residual copper (1.26 % and 2.68 %, for the lithium-poor and lithium-rich samples, respectively) and a slight excess of lithium ($x = 2.301(4)$) in the lithium-poor sample. Also, in an effort to ensure high lithium content in the lithium-rich sample, it was treated twice with excess *n*-BuLi. ICP analysis showed that the lithium-rich sample contained a significant excess of lithium, $x = 9.223(5)$. These two neutron samples are designated Li-1 and Li-2 for the low and high lithium content samples, respectively.

3. Characterization

The products were insoluble in a variety of acids even after exposure to acidic solutions for extended periods of time. Therefore, elemental analysis for chlorine, lanthanum, and niobium as well as for copper was carried out by EDS on a series of individual crystallites on a JEOL (model JSM-5410) scanning electron microscope that is equipped with an EDAX (DX-PRIME) microanalytical system. Lithium ions could be removed from the samples by deintercalation with nitric acid at 60 °C for 24 h. The resulting solutions were analyzed by ICP with a VISTA-MPX CCD Simultaneous ICP-OES analyzer. The lithium content in the intercalated product was also determined indirectly by a titration method. The amount of unreacted *n*-BuLi remaining in solution after intercalation procedures was titrated with 4-biphenylmethanol in THF dried over K/benzophenone. The titration end point was indicated by the appearance of an orange-red color in the solution [8].

Initially the lithium samples were analyzed under a stream of dry nitrogen with X-ray powder diffraction on a Philips X-Pert PW 3020 MPD X-ray diffractometer equipped with a graphite monochromator and Cu$K\alpha$ radiation ($\lambda = 1.5418$ Å). X-ray powder patterns were collected in a continuous mode between 5° and 95° 2θ with a scan speed of 0.020°/s.

Room-temperature neutron data were also collected on the lithium samples, Li-1 and Li-2. To prepare the air-sensitive samples for neutron analysis, typically 3–4 g of material were loaded into a quartz tube (9 mm outer diameter and less than 5.5 cm in length) in an argon-filled dry box. The powder was packed into the tube with a glass rod. Then 2–3 pieces of smaller diameter quartz rods were placed on top to secure the powder in place. The tube was then evacuated on a vacuum line and back-filled several times with helium. Finally, the sample was sealed with a slight pressure of helium (ca. 50–100 mTorr). Samples were

then sent to the Chalk River Laboratories, Chalk River, Ontario, Canada. The neutron powder measurements were performed on the C2 diffractometer with an 800 wire BF_3 detector that spans 80° 2θ, $\Delta = 0.1°$ 2θ, and floats pneumatically over an epoxy dancefloor. The incident wavelength of 1.32940 Å used in the Rietveld refinement was calibrated with an external Si powder. The data for both samples were collected in two separate banks from 3–83° and 37–117° 2θ with wire spacing 0.1°. Each bank was collected for 1 h. Rietveld refinement of the structure model was performed on the two sets of data simultaneously with the GSAS set of programs [9].

4. Results

4.1. Synthesis

The ability of $(CuCl)LaNb_2O_7$ to act as a host for intercalation reactions has been investigated. Treatment of this compound with strong reducing agents allows one to maintain the layers and retain chloride within the structure, but did result in the reduction of Cu^{2+} to copper metal. The reaction with *n*-BuLi can be described according to the equation:

$$(CuCl)LaNb_2O_7 + x\ n\text{-BuLi} \rightarrow (Li_xCl)LaNb_2O_7 + Cu^0 + x/2CH_3(CH_2)_6CH_3.$$

The copper metal was removed from the sample by converting it to CuI in the presence of iodine:

$$(Li_xCl)LaNb_2O_7 + Cu^0 + (x-1)2I_2 \rightarrow (Li_2Cl)LaNb_2O_7 + CuI + (x-2)LiI.$$

Also, as indicated in this equation, the initially reduced compound, $(Li_xCl)LaNb_2O_7$, was oxidized (deintercalated) to give $(Li_2Cl)LaNb_2O_7$. The CuI, and presumably any LiI, was removed by a wash step with acetonitrile. Reintercalation of lithium into $(Li_2Cl)LaNb_2O_7$ found that the compound was able to uptake lithium in the range of $2 < x < 4$ for $(Li_xCl)LaNb_2O_7$.

4.2. Structure

Neutron data were collected on the two $(Li_xCl)LaNb_2O_7$ samples, lithium-poor Li-1 and a lithium-rich Li-2 (Figs. 1 and 2, respectively). An expansion in volume occurs when more lithium is added into the structure; the *c*-axis decreases while *a*-axis increases for Li-2 relative to Li-1 (Tables 1 and 2, respectively). The starting model used in Rietveld refinement for both samples was similar to that of $(CuCl)LaNb_2O_7$ in the space group $P4/mmm$. In this model, the lithium atoms were placed in tetrahedral coordination $(0, \frac{1}{2}, z)$. In the Li-1 case, the thermal parameter for the apical oxygen was moderately high and that for niobium went negative; for subsequent refinements, the niobium thermal parameter was fixed at 0.00038. In the Li-2 refinement, a relatively high thermal parameter was obtained for the lithium. Other models were investigated where the lithium was disordered such as $(x, \frac{1}{2}, z)$, (x, x, z), or (x, y, z). The best fit however was obtained when the alkali metal sat on $4i$ position with the coordinates $(0, \frac{1}{2}, z)$. Full occupancy of this site accounts for up to only four lithium atoms in the structure. Efforts to also locate other lithium positions in this compound were not successful—this may indicate that the additional lithium is either highly disordered in the structure or is not in the compound but exists as a contaminant in the sample. Anisotropic refinements were carried out on both systems; in the case of Li-2, the improvement was significant and these data are reported in Table 3. For Li-1, no significant

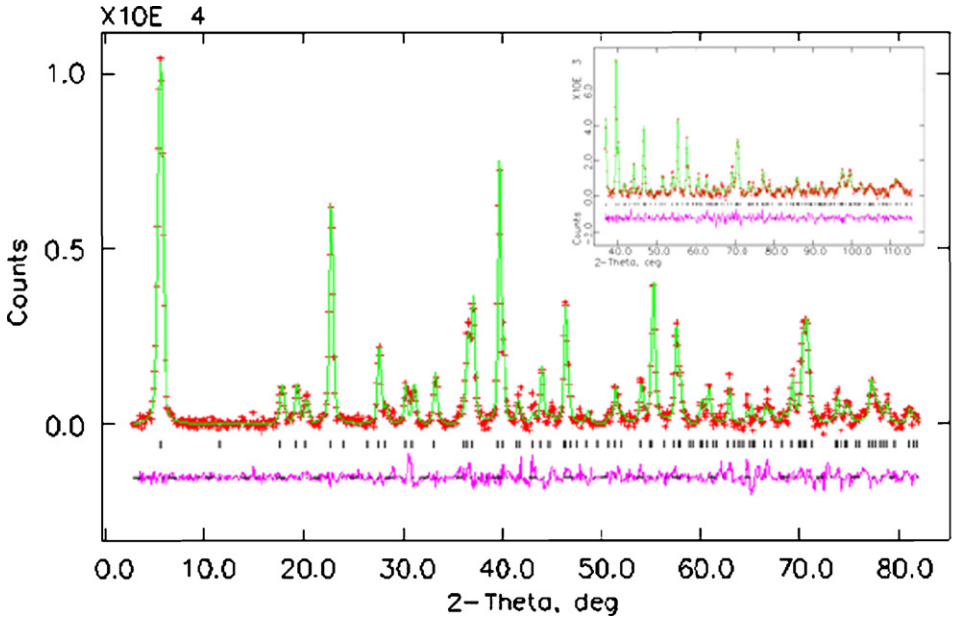

Fig. 1. Neutron diffraction data for $(Li_xCl)LaNb_2O_7$ sample Li-1. Inset is the higher-angle data for second detector.

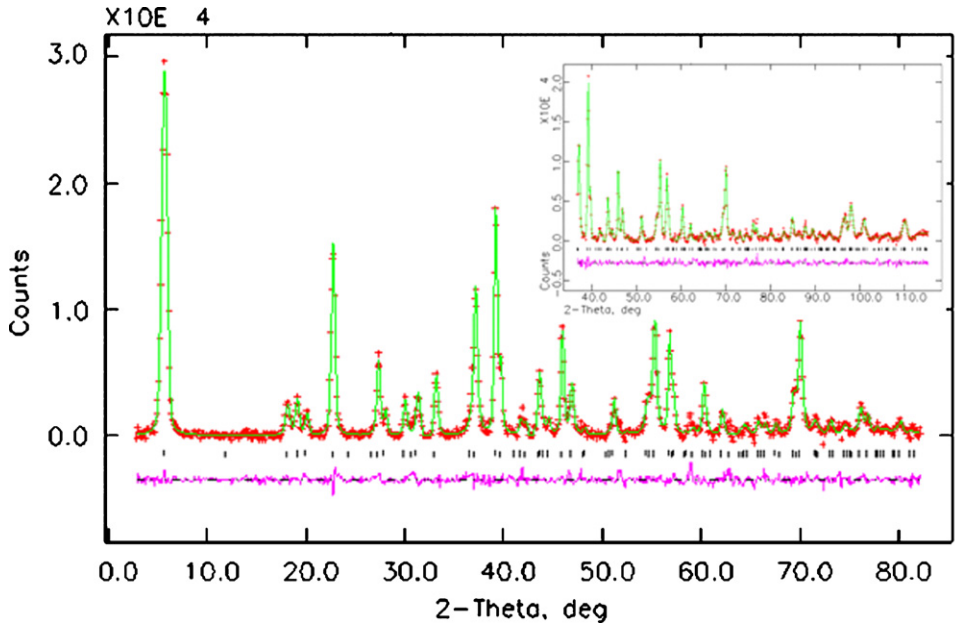

Fig. 2. Neutron diffraction data for $(Li_xCl)LaNb_2O_7$ sample Li-2. Inset is the higher-angle data for second detector.

Table 1
Crystallographic data from neutron diffraction for sample Li-1

Atom	Site	x	y	z	g	U_{iso} (Å^2)
Li	4*i*	0	$\frac{1}{2}$	0.417(5)	0.48(6)	0.0605(2)
Cl	1*b*	0	0	$\frac{1}{2}$	0.932(2)	0.0468(1)
La	1*a*	0	0	0	1	0.0057(1)
Nb	2*h*	$\frac{1}{2}$	$\frac{1}{2}$	0.1790(5)	1	0.00038
O1	4*i*	0	$\frac{1}{2}$	0.1477(6)	1	0.0250(1)
O2	2*h*	$\frac{1}{2}$	$\frac{1}{2}$	0.3196 (2)	1	0.1246(1)
O3	1*c*	$\frac{1}{2}$	$\frac{1}{2}$	0	1	0.0872(6)

*P*4/*mmm*, $Z = 1$, $a = 3.8875(3)$ Å, $c = 12.573(2)$ Å and volume = 190.01(3) Å^3, $\chi^2 = 4.21$; for low-angle data: $R_p = 2.08\%$, $R_{wp} = 2.78\%$, $R(F^2) = 7.96\%$; for high-angle data: $R_p = 2.16\%$, $R_{wp} = 2.76\%$, $R(F^2) = 6.35\%$, g = occupation factor.

Table 2
Crystallographic data from neutron diffraction for sample Li-2

Atom	Site	x	y	z	g	U_{eqv} (Å^2)
Li	4*i*	0	$\frac{1}{2}$	0.3860(3)	0.73(6)	0.1360
Cl	1*b*	0	0	$\frac{1}{2}$	0.967(2)	0.0378
La	1*a*	0	0	0	1	0.0153
Nb	2*h*	$\frac{1}{2}$	$\frac{1}{2}$	0.1762(5)	1	0.0038
O1	4*i*	0	$\frac{1}{2}$	0.1461(6)	1	0.0324
O2	2*h*	$\frac{1}{2}$	$\frac{1}{2}$	0.3227(1)	1	0.0788
O3	1*c*	$\frac{1}{2}$	$\frac{1}{2}$	0	1	0.056

*P*4/*mmm*, $Z = 1$, $a = 3.9317(2)$ Å, $c = 12.408(1)$ Å and volume = 191.81(2) Å^3, $\chi^2 = 5.52$; for low-angle data: $R_p = 1.58\%$, $R_{wp} = 2.11\%$, $R(F^2) = 2.8\%$; and for high-angle data: $R_p = 1.6\%$, $R_{wp} = 2.08\%$, $R(F^2) = 3.36\%$; g = occupation factor.

improvement was realized so only isotropic data are reported. The refinement of the site occupancies showed a slight deviation in the lithium and chlorine stoichiometry while the other atoms in the structure were essentially invariant; therefore, the occupancies of lithium and chloride were varied and those of the other atoms were fixed. Based on the refinement, the final compositions can be written as $(Li_{1.9(2)}Cl_{0.932(2)})LaNb_2O_7$ and $(Li_{2.9(2)}Cl_{0.967(2)})LaNb_2O_7$, for Li-1 and Li-2, respectively. The structure obtained for Li-1 is shown in Fig. 3. Selected bond distances are provided in Table 4, which are consistent with literature data [10].

Table 3
Anisotropic thermal parameters for sample Li-2

Atom	U_{11}	U_{22}	U_{33}
Li	0.01(2)	0.19(3)	0.20(6)
Cl	0.027(2)	0.027(2)	0.059(9)
La	0.014(2)	0.014(2)	0.017(7)
Nb	0.004(2)	0.004(2)	0.003(4)
O(1)	0.001(2)	0.011(2)	0.085(5)
O(2)	0.115(6)	0.115(6)	0.006(7)
O(3)	0.079(5)	0.079(5)	0.011(9)

5. Discussion

Reactions with the $(CuCl)LaNb_2O_7$ system have shown that copper ion is reduced to copper metal when reacted with *n*-BuLi and that on reduction the copper is replaced by lithium to produce the compound, $(Li_xCl)LaNb_2O_7$. When the lithium product is reacted with iodine, the copper impurity can be converted to CuI and this is accompanied by the deintercalation of some lithium, leading to $(Li_2Cl)LaNb_2O_7$. A reintroduction of lithium by reductive intercalation readily occurs where less than four lithiums ($x \approx 3.6$) are inserted. Rietveld refinement on neutron data of the sample with higher lithium content (Li-2) indicated a

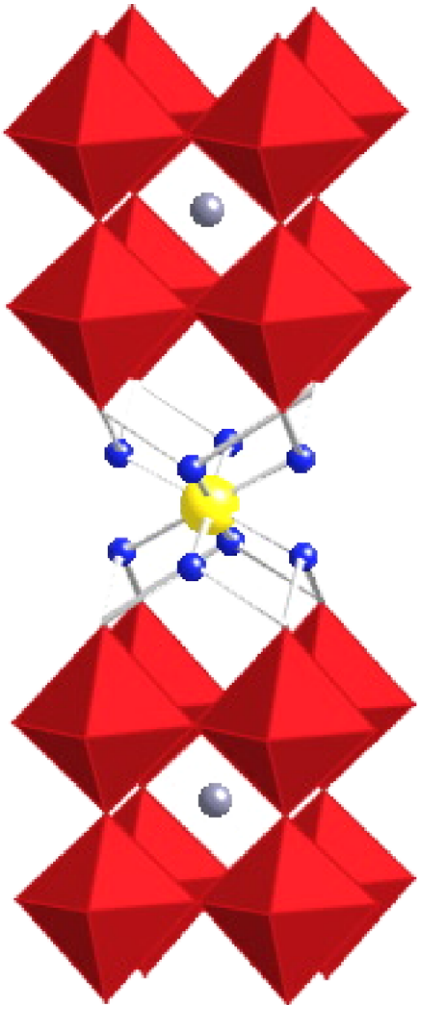

Fig. 3. Structure model for $(Li_xCl)LaNb_2O_7$ based on refinement of Li-1 neutron diffraction data. The red octahedra represent NbO_6, the gray sphere represents lanthanum, the yellow, chloride, and the blue lithium.

Table 4
Selected bond distances for Li-1 and Li-2

Bond type	Length (Å) Li-1	Length (Å) Li-2
Li–O2 × 2	2.295(3)	2.117(2)
Li–Cl × 2	2.209(3)	2.422(2)
Nb–O1 × 4	1.9833(2)	2.0011(2)
Nb–O2 × 1	1.768(2)	1.818(6)
Nb–O3 × 1	2.251(7)	2.187(6)
La–O1 × 8	2.688(5)	2.674(5)
La–O3 × 4	2.7489(2)	2.7802(6)

lithium composition of $x \approx 3$ where the lithium was found to occupy only one crystallographic site in the structure. This formulation is in disagreement with the ICP data on the Li-2 sample, which indicated $x \approx 9$. It is believed that the additional lithium was not actually taken up by the structure, but that the unusually large sample size for the neutron sample made washing the material difficult and therefore our treatment was less effective in removing any residual lithium from the intercalation step.

For the lithium-rich sample, Li-2, the refined composition indicates that the formal oxidation state of niobium is about +4.5. Previous intercalation studies on other Dion–Jacobson double-layered compounds showed that 4.5 is the lowest oxidation state achieved by niobium in these structures, though intercalation there appeared to be limited by structural considerations [2,11]. In any case, based on full occupancy of the single lithium site located by refinement of the neutron data, the lowest oxidation state achievable for niobium in this system is +4.0.

A novel layered perovskite was obtained by topotactic reactions where double lithium oxychloride arrays are constructed between sets of perovskite blocks. The basic structure consists of a set of lithium ions tetrahedrally coordinated with two apical oxygens from the perovskite strata and two chlorines from a halide layer (Fig. 3); the chlorine layer is intermediate to the two alkali-metal layers. For the lithium-rich compound (Li-2), the LiO_2Cl_2 tetrahedra are significantly distorted from the more regular tetrahedral configuration seen in Li-1, i.e., $(Li_2Cl)LaNb_2O_7$ (Fig. 4(a)). Thus, lithium ions in Li-2 form two short bonds with the apical oxygens and two long bonds with chloride ions. With respect to the NbO_6 octahedra from the perovskite layer, the octahedra become more symmetric in the lithium-rich Li-2 versus Li-1. These different effects can be seen in the relative cell constants where the *c* parameter shrinks by about 0.165 Å and the *a* parameter is slightly increased (0.044 Å) on intercalating Li-1 to form Li-2. After intercalation, both the interlayer charge and the charge of the perovskite layers are increased so that stronger interactions are expected; this is consistent with the contraction in *c*. At the same time, Nb^{5+} in Li-1, which is the subject of a second-order Jahn–Teller distortion [12], is reduced to $Nb^{4.5+}$ in Li-2 and the degree of distortion is lessened. As a result, the decrease in off-plane distortion of

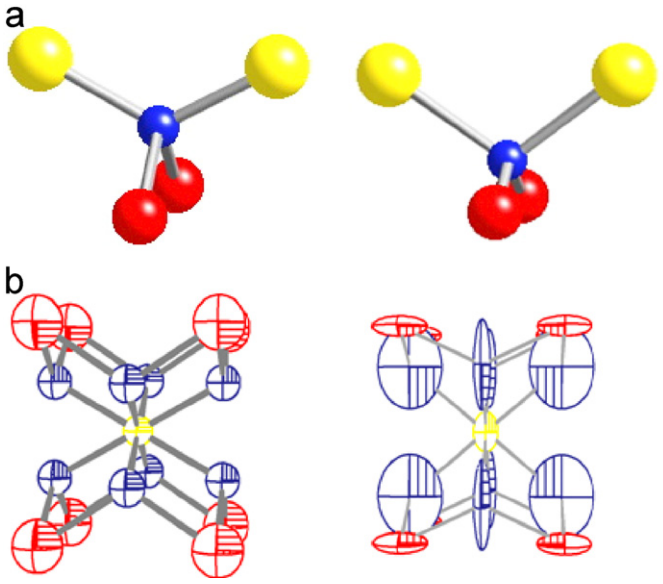

Fig. 4. (a) LiO_2Cl_2 tetrahedra for Li-1 (left) and Li-2 (right). (b) Thermal ellipsoids for Li-1 (left) and Li-2 (right). (The yellow spheres/ellipsoids represent chloride, the red oxygen and the blue lithium.)

the niobium ion for the intercalated compound translates to a small expansion in *a*-axis. Similar trends have been noted in other lithium-intercalated Dion–Jacobson compounds [13].

The anisotropic thermal refinement for Li-2 leads to lithium ellipsoids extremely elongated towards the center of four coordinate site formed by the apical oxygens of the perovskite layer (Fig. 4(b)). Since four-fold coordination is very common for lithium and taking into account the possibility of lithium mobility as observed by others in lithium-intercalated layered compounds [14], it is very possible that lithium ions have the tendency to move in the direction of the apical oxygen plane to form a square planar geometry. The displacement of the apical oxygens compensates for this behavior. In the case of Li-1, the tetrahedral environment around lithium ions is more ideal with the oxygen and chlorine bond distances of ~2.2 Å and where the slightly large thermal parameter observed for the apical oxygens might be due to the fact that only 50% of the lithium sites are occupied leading to a more disordered structure.

6. Conclusions

The use of layered perovskites as platforms for the construction of metal-anion arrays has been further demonstrated. Through the tandem use of ion exchange, to introduce the halide component, and reductive intercalation, to introduce the alkali metal, compounds with double-layer alkali-metal-halide arrays can be formed. This approach adds to the growing number of topochemical methods. As the library of such reaction strategies increases, so will one's ability to target and synthesize new solid state compounds with specifically designed features.

Acknowledgments

This material is based upon work supported by the National Science Foundation under Grant no. 0309972. Special thanks to Drs. Ian Swainson and Lachlan Cranswick of the Chalk River National Laboratories, Canada, for their assistance in the collection of neutron data. Prof. L. Spinu and Dr. B.L. Cushing are also thanked for helpful discussions.

References

[1] R.E. Schaak, T.E. Mallouk, Chem. Mater. 14 (2002) 1455.
[2] M. Sato, T. Jin, H. Ueda, Chem. Lett. (1994) 161;
K. Toda, M. Takahashi, Z.G. Ye, M. Sato, Y. Hinatsu, J. Mater. Chem. 9 (1999) 799;
R.A. McIntyre, A.U. Falster, S. Li, W.B. Simmons Jr., C.J. O'Connor, J.B. Wiley, J. Am. Chem. Soc. 120 (1998) 217;
J.N. Lalena, B.L. Cushing, A.U. Falster, W.B. Simmons Jr., C.T. Seip, E.E. Carpenter, C.J. O'Connor, J.B. Wiley, Inorg. Chem. 37 (1998) 4484.
[3] B.L. Cushing, J.B. Wiley, Mater. Res. Bull. 34 (1999) 271.
[4] L. Viciu, G. Caruntu, N. Royant, J. Koenig, W.L. Zhou, T.A. Kodenkandath, J.B. Wiley, Inorg. Chem. 41 (2002) 3385;
L. Viciu, V.O. Golub, J.B. Wiley, J. Solid State Chem. 175 (2003) 88.
[5] T.A. Kodenkandath, J.N. Lalena, W.L. Zhou, E.E. Carpenter, C. Sangregorio, A.U. Falster, W.B. Simmons, C.J. O'Connor, J.B. Wiley, J. Am. Chem. Soc. 121 (1999) 10743.
[6] T.A. Kodenkandath, M.L. Viciu, X. Zhang, J.A. Sims, E.W. Gilbert, F.-X. Augrain, J.-N. Chotard, G.A. Caruntu, L. Spinu, W.L. Zhou, J.B. Wiley, Proc. Mater. Res. Soc. Symp. 658 (2001) GG8.5.
[7] J. Gopalakrishnan, V. Bhat, B. Raveau, Mater. Res. Bull. 22 (1987) 413.
[8] B.S. Furniss, A.J. Hannaford, P.W.G. Smith, A.R. Tatchell, Vogel's Textbook of Practical Organic Chemistry, fifth ed., Longman Scientific and Technical, UK, 1989.
[9] A. Larson, R.B. Von Dreele, GSAS: generalized structure analysis system, Los Alamos National Laboratory, Los Alamos, NM, 1994.
[10] A.F. Wells, Structural Inorganic Chemistry, fifth ed., Oxford University Press, New York, 1984.
[11] A.R. Armstrong, P.A. Anderson, Inorg. Chem. 33 (1994) 4366.
[12] N.S. P Bhuvanesh, J. Gopalakrishnan, J. Mater. Chem. 7 (1997) 2297.
[13] R. Jones, W.R. McKinnon, Solid State Ionics 45 (1991) 173;
C. Bohnke, O. Bohnke, J.L. Fourquet, J. Electrochem. Soc. 144 (1997) 1151.
[14] G. Hyett, O.J. Rutt, Z.A. Gal, S.G. Denis, M.A. Hayward, S.J. Clarke, J. Am. Chem. Soc. 126 (2004) 1980.